

Green Production of Ultrahigh-Basicity Polyaluminum Salts with Maximum Atomic Economy by Ultrafiltration and Electrodialysis with Bipolar Membranes

Qing Chen,[†] Chang Xue,[†] Wei-Ming Zhang,^{*,†} Wei-Guo Song,^{*,‡} Li-Jun Wan,[‡] and Kun-Song Ma[§]

[†]College of Chemistry & Materials Engineering, Wenzhou University, Wenzhou 325000, P.R. China

[‡]Beijing National Laboratory for Molecular Sciences (BNLMS); Institute of Chemistry, Chinese Academy of Sciences, Beijing 100190, P.R. China

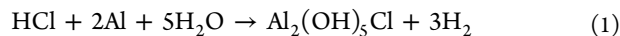
[§]Yangzhou Hongyuan Electronic Co., Ltd., Gaoyou 225600, P.R. China

S Supporting Information

ABSTRACT: Ultrahigh-basicity polyaluminum, an important aluminum industrial product, is manufactured by the oxidation of metallic Al with acids. The process is not economically and chemically efficient because the aluminum atoms were reduced first from alumina to aluminum metal and then oxidized again to get the polyaluminum. In this work, an integrated synthesis system has been built to produce ultrahigh-basicity polyaluminum salts, including polyaluminum chloride, sulfate, and nitrate, from aluminum hydroxide and corresponding acids directly at normal temperature and pressure. Ultrafiltration and electrodialysis with bipolar membranes work in tandem during the synthesis. Aluminum salts are produced naturally from aluminum hydroxide solids and acids in a mixing tank, which are separated as pure solutions via ultrafiltration and then basified in an electrodialysis stack with bipolar membranes to get polyaluminum and regenerate acids as byproducts. These acids are sent back to the mixing tank for reuse again. This integrated system works with maximum atomic economy and low overall cost, which makes it a green process for the production of polyaluminum salts.

1. INTRODUCTION

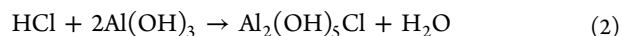
Polyaluminum salts are partially neutralized aluminum salts. Taking polyaluminum chloride (PAC) for example, the empirical formula is $Al_m(OH)_nCl_{3m-n}$ where $m \geq 1$ and $0 < n \leq 3m$. The basicity of the PAC is defined by $n/3m$, indicating the neutralization degree.^{1,2} Polyaluminum salts are broadly divided into three groups based on the basicities: low-basicity, high-basicity, and ultrahigh-basicity products. Ultrahigh-basicity polyaluminum salts, with basicities of ~65%–83%, are the products with the greatest utilities and the best commercial interests.¹ These products are generally manufactured by the oxidation of aluminum metal in the presence of aluminum salts or acids, and acids are always chosen because of the lower prices.¹ A typical reaction is shown below:



High purity products are yielded in this reaction, while the process suffers from the high cost of the aluminum metal as well as the explosion risk of the liberated hydrogen gas. It is well-known that aluminum metal is electrochemically produced from alumina by the Hall-Héroult process, and the energy requirement in this process is extremely high, which is 14 000–16 000 kWh per ton of aluminum metal.³ So the reaction in eq 1 is not economically efficient, and alternative aluminum sources are needed. In a panoramic view, the Bayer process is the cornerstone of the whole aluminum industry, which refines bauxite ore to produce aluminum hydroxide ($Al(OH)_3$, also known as alumina trihydrate or $Al_2O_3 \cdot 3H_2O$) and then alumina used in the Hall-Héroult process.⁴ Technically speaking, all

aluminum related chemicals are originated from $Al(OH)_3$, such as aluminum metal, aluminum salts, and polyaluminum salts.

The process in eq 1 is not green because the Al atoms were reduced first from alumina ore (trivalent Al) to Al metal and oxidized again to polyaluminum (trivalent Al) product. Such unnecessary atom valence variations should be avoided to achieve high overall energy efficiency. An ideal green process should be able to produce the polyaluminum salts from the $Al(OH)_3$ and corresponding acids directly as the following formula:



In this situation, chemicals with low cost and good environmental benignities are used as raw materials. All reactants are converted to the final products (plus water), which enables the best atomic economy and completely prevents the waste generation. If it could happen as wished in eq 2, this reaction certainly should be a role model of green processes.^{5,6} Unfortunately, this reaction process cannot happen directly and simply. Aluminum salts ($AlCl_3$ for example) are obtained instead of polyaluminum salts when the $Al(OH)_3$ and acid react together at normal temperature and pressure. High temperature and pressure must be involved for the industrial production of low-basicity polyaluminum salts. Gunnarsson et al. proposed a process to produce polyalumi-

Received: June 11, 2014

Revised: July 19, 2014

Accepted: August 8, 2014

Published: August 8, 2014

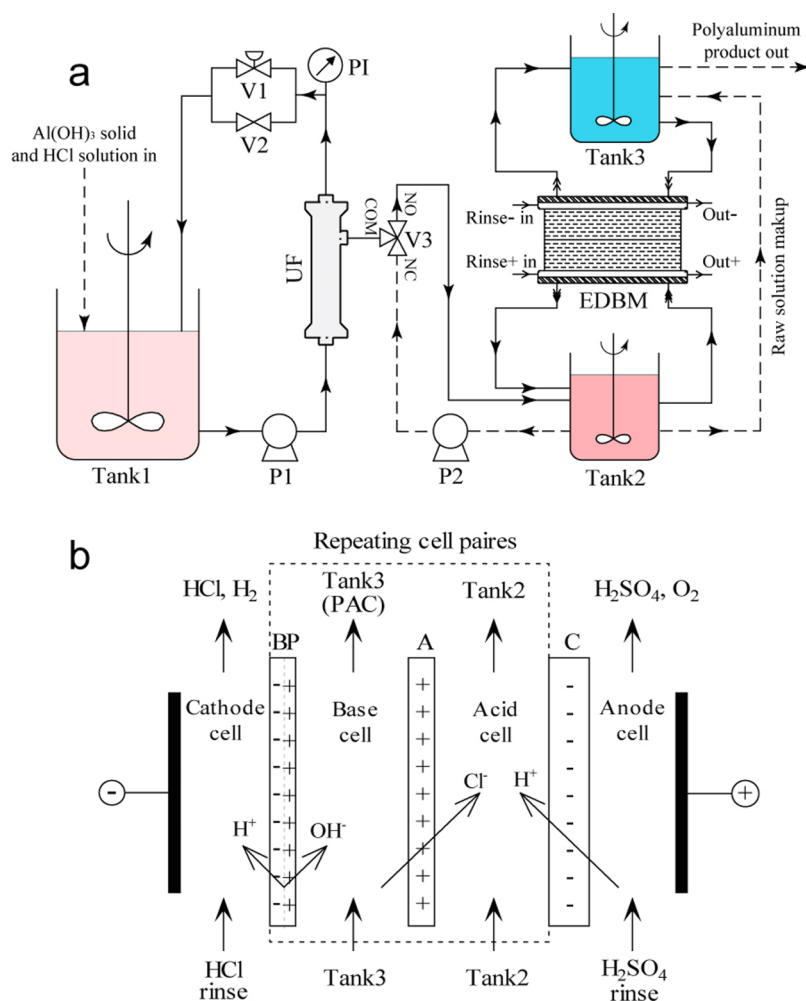


Figure 1. (a) Simplified process diagram of the integrated UF-EDBM system. (b) Detailed illustration of the EDDBM stack. Tank1, mixing tank for Al(OH)₃ and acid; Tank2, tank for UF permeate exchange and EDBM acid receiving; Tank3, tank to receive polyaluminum products; P1, UF recirculation pump; P2, UF back-flush pump; V1, manual throttle for UF pressure adjustment; V2 and V3, solenoid valves; PI, pressure indicator; C, cation exchange membrane; A, anion exchange membrane; BP, bipolar membrane.

num salts from Al(OH)₃ and corresponding acids by heating their mixture to a temperature of 180–220 °C in closed containers (~1.0 MPa pressure) using microwaves, and the highest product basicity was about 45%.⁷ Due to the corrosive nature of the reactants and the cost of operation at high pressure, this process is far from satisfactory. Furthermore, it is difficult to obtain products with higher basicities, even in more severe temperature and pressure conditions because of the kinetic nature of the aluminum solution chemistry.^{8–10} Partial thermal decomposition (~260 °C) of AlCl₃·6H₂O is another possible route to get polyaluminum chloride,^{11,12} but the product purity and quality are insufficient for high-end uses.

Many efforts have been made to provide alternative processes for industrial production of ultrahigh-basicity polyaluminum salts,^{1,2,9,13–15} among which the electrodialysis with bipolar membranes (EDBM) method shows the best energy and economy efficiencies.^{1,13} EDBM is an electro-membrane process combining the conventional electrodialysis and water splitting in bipolar membranes, and it can convert the salt into corresponding acid and base without involving any impurities.^{16–18} It has been well proven in our previous work that the EDBM process can convert the aluminum salt to ultrahigh-basicity polyaluminum salt (up to 74% basicity) and corresponding acid.¹³ Here in this work, we propose a novel

system which integrates the ultrafiltration (UF) and EDBM modules to work in tandem and makes the process in eq 2 happen smoothly at normal temperature and pressure. In this novel process, aluminum salts are produced naturally from aluminum hydroxide solids and acids in a mixing tank. They are separated as pure solutions via UF and then basified in an EDBM stack to get polyaluminum and regenerate acids as byproducts. These acids are sent back to the mixing tank and recycled. During the process, only acid solutions and aluminum hydroxide solids are used as the feed stocks; polyaluminum solutions are produced without any waste generation. This integrated system is promising as a greener process for the future industrial production of polyaluminum salts, especially for the ultrahigh-basicity products.

2. EXPERIMENTAL SECTION

2.1. Kinetics of Al(OH)₃ Dissolving in Acids. The kinetics of Al(OH)₃ dissolving in acid was investigated by jar tests. Several Al(OH)₃ solids from different suppliers were evaluated. Al(OH)₃ powder (50.0 g) was dispersed in distilled water under stirring to form a milk-like slurry (900 mL) in a jacketed jar. The temperature of the slurry was kept at 30 ± 0.5 °C. Concentrated (~37 wt %) HCl (43.6 g) was diluted to 100

mL. The dilute HCl was added to the slurry quickly, and the reaction began. Samples were taken at predetermined intervals to monitor the remaining H^+ concentrations in the reactor. All samples were centrifuged and filtrated immediately (by 0.2 μm pore size membranes) to remove all suspending $\text{Al}(\text{OH})_3$ particles.

2.2. System Setup. Simplified process diagram and photographs of the integrated UF-EDBM system are shown in Figure 1a and Figure S1, respectively. A hydrophilic PVC hollow fiber UF module (the first stage of LUSA-CU-1C UF system, from Hainan Litree Purifying Technology Co., Ltd., China) was used in this system. The outer diameters of membrane fibers are 1.6 mm, and inner diameters are 1.0 mm, and the total membrane area is about 0.2 m^2 . The molecular weight cutoff (MWCO) of the fiber is 50 000 Da, and the pore size is 0.01 μm . The detailed configuration of the EDBM stack is shown in Figure 1b. It has a two-compartment configuration with cocurrent flows, which consists of alternating bipolar membranes (BPs, Fumasep FBM from FuMA-Tech GmbH, Germany) and anion exchange membranes (AEMs, Selemion AMT from Asahi Glass Engineering Co., Ltd., Japan). There are nine repeating cell pairs in the stack. Heavy CEM (Selemion CMD also from Asahi Glass Engineering Co., Ltd., Japan) is selected as the anode membrane, because it has excellent resistance to the oxidant (such as O_2 and Cl_2) generated on the anode surface. HCl solution (0.50 mol/L) was chosen as the catholyte rinse to avoid anion contaminations, and H_2SO_4 solution (0.25 mol/L) was chosen as the anolyte rinse to eliminate toxic Cl_2 gas emission. The EDBM stacks were designed and homemade in our lab, equipped with a homemade spacer with a dimension of 260 mm (length) \times 130 mm (width) \times 0.9 mm (thickness). The spacer consists of a polyethylene (PE) sheet and polypropylene (PP) turbulence accelerating mesh net, with a tortuous flow path of 33 mm (width) \times 567 mm (length), i.e. 187 cm^2 of effective area. The detailed drawing of the spacer as well as characteristics of the above membranes can be found in our previous work.¹³

2.3. Operation Protocols. The $\text{Al}(\text{OH})_3$ solids and acid solution were mixed in a large mixing tank (Tank1) to form a suspension. Then the slurry was recirculated (driven by P1, DP-130 diaphragm pump) through the UF hollow fibers, and the back pressure in the UF module was adjusted by a throttle (V1). The slurry was filtrated in a cross-flow mode, and the resulting permeate was sent to the acid tank (Tank2), where the liquid level rose gradually. When it reached a specific high level, the solenoid valves (V2 and V3) and the back-flush pump (P2, DP-100 diaphragm pump) were energized. During this period, permeate in Tank2 was drawn back and the UF module was flushed for flux recovery. The liquid level dropped until it reached a specific low level. All above operations were accomplished automatically by a programmed logic controller (PLC, TECO SG2-20HR).

The integrated system worked in a batch mode. When most of the free H^+ was neutralized, the liquids in Tank1 and Tank2 were basically aluminum salt solutions. The feed solution in the base tank (Tank3) was supplied from Tank2, and this solution will be replenished by UF automatically. After Tank3 was filled, the EDBM subsystem started running as illustrated in Figure 1b. The aluminum salt solution in Tank3 was basified to get polyaluminum salt products, and the acid accumulated in Tank2. During this process, the solutions in Tank2 and Tank1 were exchanged freely via the UF subsystem. The acid in Tank2 was sent to Tank1, where it was neutralized by $\text{Al}(\text{OH})_3$, and

the resulting solutions were sent back to Tank2. After this EDBM basification process, extra $\text{Al}(\text{OH})_3$ solids and acid solutions were added to Tank1 to compensate the material loss for a new batch of running.

2.4. Analytical Methods. The total Al concentrations in samples were analyzed by inductively coupled plasma optical emission spectrometry (ICP-OES, PerkinElmer Optima 8000). The H^+ and Cl^- concentrations were determined by potentiometric titration (INESA ZDJ-4B automatic titrator), with 0.10 mol/L NaOH and 0.10 mol/L AgNO_3 standard solutions.

The alkalinity (defined as $[\text{OH}^-]'$) of the polyaluminum sample was analyzed by neutralization of alkalinity with excess acid and back-titration with NaOH in the presence of KF.¹⁹ The basicity of the polyaluminum sample can be calculated as follows:^{1,2}

$$\text{Basicity} = \frac{[\text{OH}^-]'}{3[\text{Al}_t]} = \frac{[\text{OH}^-]'}{[\text{OH}^-]' + [\text{X}^-]} \quad (3)$$

where $[\text{OH}^-]'$ is the concentration of hydroxyl coordinating with aluminum in the sample, $[\text{Al}_t]$ is the total aluminum concentration, and $[\text{X}^-]$ is the total equivalent concentration of all anions (such as Cl^- , NO_3^- , or $1/2\text{SO}_4^{2-}$).

The cumulative current efficiency η in the EDBM process is calculated from the amount of hydroxyl generated in product solutions:

$$\eta = \frac{[\text{OH}^-]_t' V_t - [\text{OH}^-]_0' V_0}{Q_t} = \frac{[\text{X}^-]_0 V_0 - [\text{X}^-]_t V_t}{Q_t} \quad (4)$$

where V is the volume of the product solution and Q is the cumulative charge transferred in moles of electrons. The subscripts "0" and "t" represent the sampling points, namely "before the test" and "at sampling point t," respectively.

3. RESULTS AND DISCUSSION

3.1. Screening of $\text{Al}(\text{OH})_3$. Theoretically $\text{Al}(\text{OH})_3$ solids are soluble in various acids and alkalis. However, the $\text{Al}(\text{OH})_3$'s obtained from the Bayer process are crystalline forms, and their reaction rates are typically slow in both acids and alkalis under normal temperature and pressure conditions, which depend on the particle size and the surface morphology. Kinetics data of four different $\text{Al}(\text{OH})_3$'s, marked as $\text{Al}(\text{OH})_3$ A, B, C, and D, are shown in Figure 2a. It is clear that the remaining H^+ concentrations are decreased in all experiments, which indicates that the free H^+ reacts with all $\text{Al}(\text{OH})_3$ solids. The reaction rates are very different; $\text{Al}(\text{OH})_3$ D reacts with acid much faster than other candidates. Generally speaking, the reaction rate of $\text{Al}(\text{OH})_3$ and H^+ at constant temperature depends on the concentration of H^+ as well as surface area of $\text{Al}(\text{OH})_3$ solids in the reactor. In our situation, we dosed much more $\text{Al}(\text{OH})_3$ solid (~ 1.9 eq/L) than H^+ (~ 0.4 eq/L). Because only a small portion of the solids dissolves during single batch, the total surface area of solids was nearly constant. It is reasonable to suppose the above reaction follows the pseudo-first-order rate law as follows:

$$\ln([\text{H}^+]_t) = -kt + \ln([\text{H}^+]_0) \quad (5)$$

where $[\text{H}^+]_t$ is the remaining H^+ concentration in the reactor at the sampling point, $[\text{H}^+]_0$ is the initial H^+ concentration, t is the corresponding reaction time, and k is the rate constant. The determination of the rate constants for different $\text{Al}(\text{OH})_3$ solids is shown in Figure 2b. The linearity in all experiments confirms

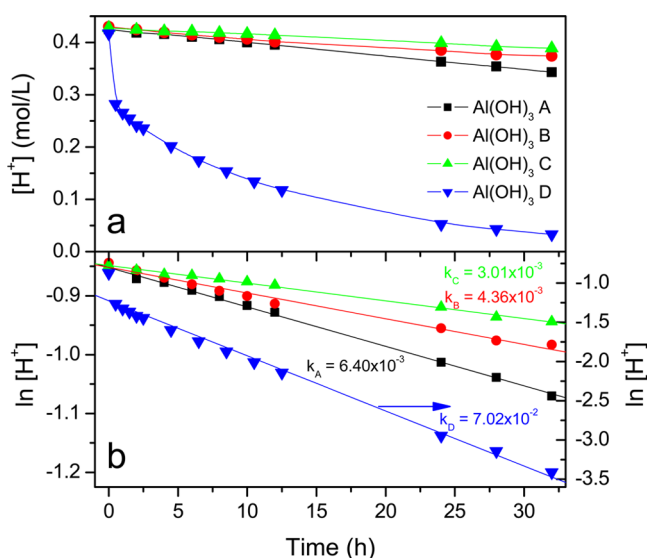


Figure 2. Kinetics of various Al(OH)_3 dissolving in acid solutions. (a) The remaining H^+ concentration plots. (b) Determinations of kinetic data. Rate constants of all Al(OH)_3 solids are calculated by the slopes of the fitted lines.

the pseudo-first-order reaction hypothesis. Rate constants of all Al(OH)_3 solids are calculated by the slopes of the fitted lines, which are also marked in Figure 2b. The half-lives of H^+ in different reactions are readily calculated from the rate constants, which are 103, 159, 230, and 9.9 h for Al(OH)_3 A, B, C, and D, respectively. So, Al(OH)_3 D is selected as the Al(OH)_3 source for our investigations, which is a commercial product with better acid solubility from a modified Bayer process.²⁰ This kind of Al(OH)_3 contains a small amount amorphous phase which reacts with acid very fast and consequently causes the deflection of the first point in Figure 2b.

It is worth mentioning that faster reaction rates are available for amorphous Al(OH)_3 products, which are also known as aluminum hydroxide gels. These products are typically used as pharmaceutical antacids because of their excellent acid-neutralizing capacities (see the U.S. Pharmacopoeia for details). However, these gels are prepared by the reaction of aluminum salts with alkalis in well controlled reactors,²¹ which are not the origin of the aluminum chemicals and suffer from high costs. So Al(OH)_3 D from the Bayer process is still the final choice in our study.

3.2. System Commissioning. $\text{AlCl}_3 \cdot 6\text{H}_2\text{O}$ solids were used directly for the system startup instead of Al(OH)_3 and HCl for a much faster start-up. About 1.9 kg of $\text{AlCl}_3 \cdot 6\text{H}_2\text{O}$ and 12 L of water were added to Tank1 under continuous stirring, and a transparent solution was formed. Al(OH)_3 powder (500 g, Al(OH)_3 D, 200 meshes) was added to the solution carefully to obtain a milk-like slurry. And then extra water was added to the solution to get 14.0 L of slurry in the mixing tank. After the slurry was well dispersed, the UF subsystem was turned on. The slurry was pumped through the UF module and returned to the mixing tank. The back pressure in the module was carefully adjusted to 0.10 MPa, and the corresponding recirculation flow rate was 1.3 LPM. The permeate filled Tank2 gradually, which appeared as a totally transparent solution. Permeation flux decreased to about 0.10 LPM as the liquid level reached the high level, indicating that thin filter cake formed in the UF fibers. After the liquid level reached the high level, a back flush procedure started automatically, and this restored the

permeation flux to about 0.15 LPM. While working in this intensive back flush mode, the flux was stabilized in the range of 0.10 LPM to 0.15 LPM. After the system was stabilized, 2.0 L of permeated solution was transferred from Tank2 to Tank3, and this part of the solution would be filled again automatically in Tank2. After all above operations, the total volume of the remaining slurry in Tank1 was about 10.0 L with a suspension solid of 5% in weight, and both Tank2 and Tank3 were filled with 2.0 L of ~ 0.50 mol/L AlCl_3 solutions.

The EDBM subsystem was started after solutions were ready in all tanks. The flow velocity in the stack was maintained at 2.5 cm/s (400 mL/min for both Tank2 and Tank3 circuit in our nine cell-pair stack). The Al ions in base cells reacted with OH^- (from H_2O splitting in bipolar membranes) to get polyaluminum salt. Parts of X^- passed through the anion exchange membranes, and then corresponding acid accumulated in the acid cells. During this process, the solutions in Tank2 and Tank1 were exchanged straightway via the UF subsystem. The accumulated acid in Tank2 was sent back to Tank1, neutralized by Al(OH)_3 , and recirculated to Tank2.

After this EDBM basification process, polyaluminum salt product was obtained by drain from Tank3. And then the Tank3 circuit was rinsed with 1 L of 1.0 mol/L HCl solution for 30 min. After this clean procedure, all used HCl was transported to Tank1. Then, 78 g of Al(OH)_3 solids and extra water were added to Tank1 until the total volume reached 12.0 L. After stirring overnight, Tank3 was filled with UF permeate again (from Tank2), and the system was ready for a new batch. Four consecutive batches (Runs 1–4) were carefully investigated in this study.

3.3. Online Data Profiles. Key parameters in the EDBM basification process, including stack voltage and current, product pH, and temperature, were monitored by a homemade control system online.² Meanwhile samples were taken at predetermined intervals for off-line analysis. All online data profiles are plotted in Figure 3. The EDBM stack is operated

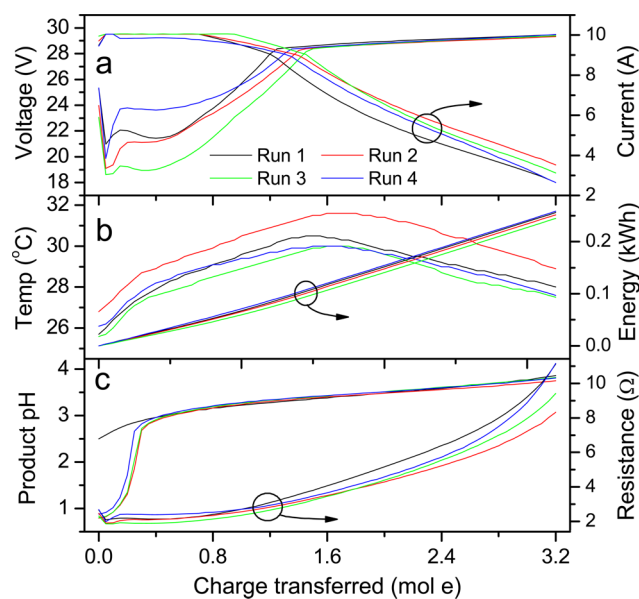


Figure 3. Online data profiles of the EDBM process. (a) Stack voltage and current curves. (b) Solution temperature curves in product solution (Tank3) and the EDBM energy consumptions. (c) The product pH and stack resistance variations. Samples were taken at charge-transfer intervals of 0.8 mol electrons.

with a limiting applied potential of 30 V, and the stack currents are limited within 10 A (53.5 mA/cm^2) in all tests. As shown in Figure 3a, the initial stack currents are all 10 A, and the corresponding voltages are in the range of 19–24 V, which is determined by the solution temperature and surface scaling status of the membranes. The voltages gradually increase to 30 V, and then the currents start to decrease, indicating stack resistance rises (also shown in Figure 3c). The temperatures of the product solutions (Tank3) are presented in Figure 3b. Tank2 and Tank3 are connected with a tap water heat exchanger to stabilize the solution temperatures (see Figure S1b for details). The stack powers are high ($>200 \text{ W}$) and the recirculation solution volumes are small (2.0 L each), so the solution temperature would soar if no heat exchanger is employed. The temperatures have been stabilized between 26 and $31 \text{ }^\circ\text{C}$ in all tests, which is similar to that in previous jar tests for $\text{Al}(\text{OH})_3$ screening. The energy consumptions are also recorded (Figure 3b), which are readily calculated from the stack voltage and current (versus time) profiles. The total energy is about 0.25 kWh for each batch, and the corresponding yield is 0.101 kg (calculated as $\text{Al}_2(\text{OH})_{4.2}\text{Cl}_{1.8}\cdot 2\text{H}_2\text{O}$ solid). The pH variations of the product solutions (Figure 3c) increase as expected in all tests. The initial pH is 2.50 in the first running because pure AlCl_3 salt is used to commission the system, and then pure aluminum salt solutions are filled in both Tank2 and Tank3. The pH increases gradually as this solution is basified. The final pH is 3.86 when the charge transferred in the stack reaches 3.2 mol electrons, which indicates the formation of ultrahigh-basidity polyaluminum salt. The initial pHs are about 0.8 in all consecutive batches, which is caused by the residual H^+ ($\sim 0.05 \text{ mol/L}$) in the slurry (Tank1). The final product pHs of these tests are nearly the same (~ 3.80) as the first running. The stack resistance profiles are also presented in Figure 3c. The initial resistance is about 2 ohm and increases to 10 ohm maximum in the EDBM processes in all tests. As described in our previous work,¹³ ion concentration depletion as well as the initial $\text{Al}(\text{OH})_3$ scaling on bipolar membrane surfaces in base cells cause the resistance soaring. The stack resistance as well as pH change patterns are very similar in all of these batches, indicating steady state operations are achieved in the integrated system.

3.4. Offline Sample Analysis. The volumes of product solution shrink during the EDBM process, which are shown in Figure 4a. These volume decreases are mainly caused by electro-osmosis.¹³ Water molecules are dragged by anions to permeate together through the AEMs in the stack. Another minor reason is the water splitting within the bipolar membrane. About 180 mL of water is moved from Tank3 to Tank2 through the membranes as the charge transferred reaches 3.2 mol electrons. $[\text{Al}_t]$ increases in Tank3 as the solution volumes shrink, which is also shown in Figure 4a. The total amounts of Al species nearly keep constant in all tests, indicating very little aluminum leakages between the acid and base cells in the stack. $[\text{Al}_t]$ in the first running is slightly higher than that in the consecutive tests, which is caused by our system operation protocol. We are trying to keep constant $[\text{Cl}^-]$ by adding equivalent HCl before the subsequent batch (also shown in Figure 4b), while part of the free H^+ still remains before the next running ($\sim \text{pH } 0.8$). Namely, H^+ substitutes little part of Al^{3+} during consecutive runnings and causes $[\text{Al}_t]$ to decrease slightly. Since the remaining $[\text{H}^+]$ nearly keeps constant in all consecutive tests, the $[\text{Al}_t]$ change patterns stay nearly the same.

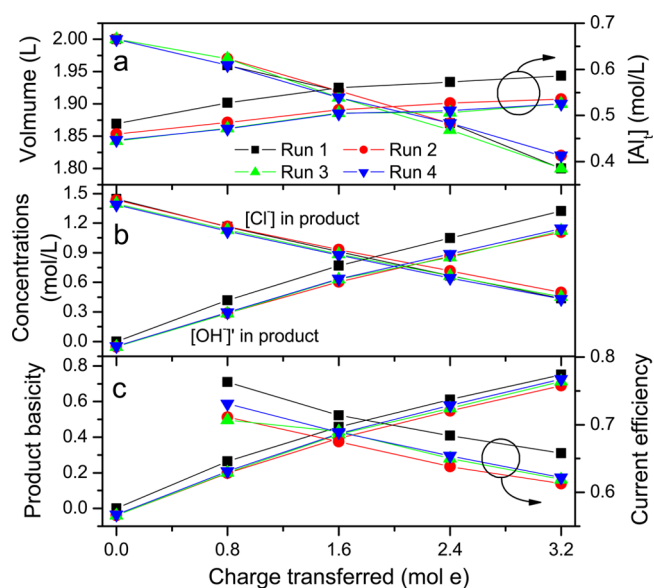


Figure 4. Offline sample analysis results in Tank3 during the EDBM process. (a) Volume and total aluminum concentration variations of the product solutions. (b) Concentration variations of Cl^- ions and hydroxyl coordinating with aluminum. (c) Variations of product basicities and cumulative current efficiencies.

During the EDBM basification process, water is split in the bipolar membranes, and the generated OH^- substitutes part of the Cl^- in the product solution, as shown in Figure 1b. Therefore, $[\text{Cl}^-]$ decreases and $[\text{OH}]'$ (concentrations of OH^- coordinating with Al) increases (Figure 4b). The Cl^- change patterns are nearly the same in all tests, which suggests good system reproducibility and stability. The $[\text{OH}]'$ in the first running (Run 1) is slightly higher than that in the consecutive tests, which is also caused by the operation protocol. Pure AlCl_3 was used for the system commissioning, while in consecutive tests the startup materials were AlCl_3 and HCl (small amount) mixtures, which caused lower $[\text{OH}]'$ patterns. As the $[\text{Cl}^-]$ increases and $[\text{OH}]'$ decreases, the basicities of polyaluminum solutions increase, which are calculated readily by eq 3 and shown in Figure 4c. The basicities of final polyaluminum salts are between 70% and 75% in all tests, which are well qualified as ultrahigh-basidity products. Very similarly, the product basicity increases from 0 to 75% in the first running, which is slightly higher than that in consecutive batches (runs 2, 3, and 4, from -4% to 70%). The cumulative current efficiencies at all sampling points in all EDBM tests are calculated by eq 4, and the results are also plotted in Figure 4c. Because of the H^+ accumulation in Tank2, the current efficiencies slightly decrease from about 72% to 62% in all tests. The increasing $[\text{H}^+]$ in acid cells of the stack lead to H^+ back diffusion to base cells, which is the opposite of the basification process.¹³

Samples are also taken in Tank2 at the same intervals to better understand the EDBM process, and the analysis results are shown in Figure 5. Because the EDBM basification process is relatively faster (about 80 to 90 min for single batch) than the neutralizing reaction of $\text{Al}(\text{OH})_3$ and H^+ (9.9 h half-life for H^+ and 24 h for single batch), the immediate H^+ neutralization during the EDBM process only takes a small part in the overall reaction in Tank1. The theoretical increase of $[\text{Cl}^-]$ in Tank2 can be estimated from the decrease of that in Tank3 by combining Tank1 and Tank2 as a whole, which is shown in Figure 5a as a dashed line. The actual $[\text{Cl}^-]$ variations are also

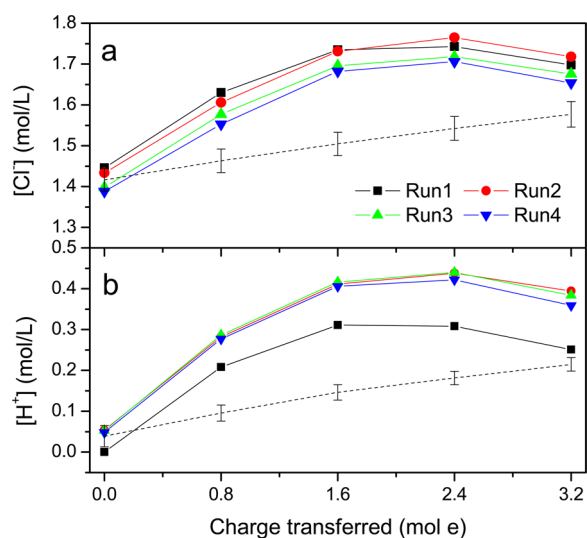


Figure 5. Offline sample analysis results in Tank2 during the EDBM process. Concentration variations of Cl^- (a) and free H^+ (b) ions are presented. The theoretical ion concentrations with infinite UF permeate exchanges are shown as dashed lines.

plotted, and they are higher than the theoretical line. Cl^- 's are moved from Tank3 to Tank2 in the EDBM stack, meanwhile a solution with increased $[Cl^-]$ in Tank2 is exchanged with Tank1 via the UF subsystem. The concentration variations are the combination of these two simultaneous subprocesses. At the initial stage of the EDBM basification process, the stack current is very high (10 A, namely 53.5 mA/cm²), which means that at this time, Cl^- electromigration is dominant, and the $[Cl^-]$ builds up quickly from 1.45 mol/L to 1.75 mol/L. While the stack current drops to less than 5 A later, the UF process impacts more and leads to the $[Cl^-]$ decrease. The $[H^+]$ in Tank2 varies in the same manner as $[Cl^-]$ above (as shown in Figure 5b), which is also regulated by these two opposite subprocesses. The peak $[H^+]$ is only 0.44 mol/L here. The free UF permeate exchange as well as the big volume of the external mixing tank hugely hinder the $[H^+]$ growing in Tank2, which is essential to maintain the reasonable current efficiencies (>62%).

3.5. Aluminum Solution Chemistry. The solution chemistry of $Al(OH)_3$ reacting with free acids is represented in Figure S2. The basic units of $Al(OH)_3$ are six-member rings of aluminum octahedrons, and these rings are combined by double hydroxide bridges (shown in Figure S2a,b).^{22,23} When attacked by protons, these combined hydroxide bridges are taken apart to form separate $[Al(H_2O)_6]^{3+}$ octahedrons directly (Figure S2b,c), which are the existence forms of Al^{3+} in aqueous solutions. Therefore, the direct reaction presented in eq 2 is not kinetically favored. Octahedral dimeric cations such as $Al_2(OH)_2(H_2O)_8^{4+}$ may be produced when high temperature and pressure are involved, and that is the principle of industrial production of low-basicity polyaluminum.⁷ While the molecular structure is quite different in ultrahigh-basicity polyaluminum salts. It is well-known that the ϵ - Al_{13} polycation ($[AlO_4Al_{12}(OH)_{24}(H_2O)_{12}]^{7+}$) with a Keggin structure is the dominated Al species in this product.^{2,8–10} Al_{13} is the highest basicity polyaluminum product of commercial interest, and it is widely used in water purification, catalysts, and cosmetics. The Al_{13} polycation has a central Al atom in a tetrahedral environment, which is surrounded by 12 Al atoms in octahedral

environments. The tetrahedral Al atoms only form in alkaline solutions. In the traditional oxidation process, aluminum metal reacts with water (the free H^+ concentration is very low when polyaluminum start to form) violently; the H^+ 's (from dissociation of water) are quickly converted to H_2 gas. It causes a high local OH^- concentration near the metal surface and results in the initial formation of tetrahedral Al atoms. As the tetrahedral Al atoms diffuse away from the metallic aluminum surface, they have good chances to coordinate other Al octahedrons to form Al_{13} .⁸ However, there is no reaction pathway to produce tetrahedral Al atoms in the direct reaction of $Al(OH)_3$ and acids, so Al_{13} species are not available in this synthesis route even if the most severe temperature and pressure conditions are involved.

In our integrated system, octahedral Al atoms form in the mixing tank by reacting of $Al(OH)_3$ and acids, and these octahedral Al atoms are transferred to Tank3 as pure solutions and recirculated in the base cells of the EDBM stack. As shown in Figure 1b, water molecules are dissociated in the bipolar membranes, and the produced OH^- migrates to these base cells. The high local OH^- concentration near the membrane surfaces is essential for the initial formation of tetrahedral Al atoms, which is very similar to the oxidation process.²⁷ Al -NMR technology is used to analyze the Al configurations in the final products in all batches, and the results are shown in Figure S3. The free octahedral Al atoms produce 0 ppm standard signals. The central tetrahedral Al atoms in Al_{13} polycations produce a 63.5 ppm resonance, and the 12 surrounded octahedral Al atoms give no signal in this configuration.² The Al_{13} species is observed in all products as 63.5 ppm resonances in Figure S3, which further confirms the formation of ultrahigh-basicity products. The Al species distribution (ratio of Al_{13} polycations and free octahedral Al ions) can be also calculated from the intensities of the 0 and 63.5 ppm peaks,² which is accorded well with the basicities in Figure 4c.

3.6. Scaling Risk and Abatement Strategy. The $Al(OH)_3$ scaling on bipolar membrane surfaces in base cells is the main risk for achieving long-term system stability, which is also the root cause for the stack resistance soaring in Figure 3c. This risk cannot be avoided because OH^- and $Al(H_2O)_6^{3+}$ contact directly on the membrane surfaces. Fortunately, this initial $Al(OH)_3$ scaling is an amorphous phase (same as $Al(OH)_3$ gel production) and can readily dissolve in dilute acids.²¹ After each batch of production, HCl solution and $Al(OH)_3$ solid must be added to Tank1 to make up for the material loss in products. This acid solution is the very cleaner for the initial amorphous $Al(OH)_3$ scaling, and it is recirculated in base cells (Tank3) for 30 min before being transported to Tank1. As shown in Figure 3c, the stack resistance increases from about 2 ohm to 10 ohm maximum in each batch, and the resistance recovers to 2 ohm again after the cleaning. This routine clean procedure greatly abates the scaling risk and ensures long-term system stability.

3.7. Brief Cost Estimation. The cost of polyaluminum production depends on the overall cost, the equipment lifespan, and process capacity. The overall cost consists of capital cost (for the system modules and peripheral equipment) and operational cost (including energy consumptions and maintenance). The most expensive component in the system is the EDBM stack, which suffers from the high cost as well as limited lifespan of the ion exchange membranes inside. In our integrated system, routine clean procedures with HCl after each batch greatly abate the $Al(OH)_3$ scaling risk and promise

an optimistic lifetime (2 years for cost estimation here) for the stack. The process capacity is mainly limited by two factors, the EDBM capacity and the reaction rate of $\text{Al}(\text{OH})_3$ with acid. It takes 2 h for EDBM operation (80–90 min for EDBM basification, and 30 min for HCl cleaning) and 24 h for the H^+ neutralization in single batch. Obviously, the latter is the bottleneck in our current system. This limitation can be overcome simply by increasing the volume of the mixing tank from 10 to 120 L, which would increase the resident time of $\text{Al}(\text{OH})_3$ and H^+ proportionally. The UF capacity will remain unchanged, and the cost increase will be limited. The detailed cost estimation is presented in Table S1 in the Supporting Information. It shows that the overall production cost for polyaluminum salts (70% basicity) from $\text{Al}(\text{OH})_3$ solids and HCl solutions is \$1.06/kg (calculated as $\text{Al}_2(\text{OH})_{4.2}\text{Cl}_{1.8}\cdot 2\text{H}_2\text{O}$ solids, \$0.77/kg for capital cost and \$0.29/kg for energy cost, cost of feed chemicals is not included) based on a 2-year system lifespan. The capital cost, especially the high cost of the ion exchange membranes, dominates the overall cost, which is promising to be reduced remarkably once a longer system lifetime can be achieved. The overall cost will be lowered to \$0.84/kg (\$0.56/kg for capital cost) and \$0.67/kg (\$0.38/kg for capital cost) based on 3-year and 5-year system lifetime estimations, respectively. The polyaluminum from this integrated system are inherently pure products, which are not contaminated with any impure ions and byproduct salts. This polyaluminum salts with high purities and ultrahigh basicities are of great commercial interest, making the integrated process proposed in this study a competitive production method. Furthermore, the polyaluminum industry will benefit tremendously from the green nature of this technology, and it is able to reduce the total carbon footprint of the polyaluminum industry significantly.

4. CONCLUSION

Ultrahigh-basicity polyaluminum salts are usually produced by the oxidation of aluminum metals in acids at elevated temperatures. This process is not satisfying because of high costs as well as large carbon footprints. In the current work, an integrated system is proposed and built to produce ultrahigh-basicity polyaluminum salts directly from $\text{Al}(\text{OH})_3$ and acid solutions. The $\text{Al}(\text{OH})_3$ raw materials are carefully screened, and operation protocols are seriously developed. In this new process, UF and EDBM work in tandem to convert $\text{Al}(\text{OH})_3$, a Al source with a lower cost and better environmental benignity, to polyaluminum salts directly with the best atom economy. The overall production steps are greatly shortened in this new process. Continuous tests on the lab system indicate this process has good robustness and repeatability, which ensures a reasonable system lifetime. The overall production cost is \$1.06/kg as polyaluminum solids (with 70% basicity), in which the energy cost is \$0.29/kg and the capital cost is \$0.77/kg. The cost-effective and green nature of this new process makes it a superior production method for the polyaluminum industry.

■ ASSOCIATED CONTENT

Supporting Information

Detailed photographs of the integrated UF-EDBM system (Figure S1), solution chemistry of $\text{Al}(\text{OH})_3$ reacted with free acids (Figure S2), ^{27}Al -NMR spectrum of the final polyaluminum products (Figure S3), and the cost estimation procedure (Table S1). This material is available free of charge via the Internet at <http://pubs.acs.org/>.

■ AUTHOR INFORMATION

Corresponding Authors

*Tel.: +86 577 86689300. E-mail: weiming@iccas.ac.cn.

*Tel.: +86 10 62557908. E-mail: wsong@iccas.ac.cn.

Notes

The authors declare no competing financial interest.

■ ACKNOWLEDGMENTS

The authors are grateful for financial support by the National Natural Science Foundation of China (Project No. 21203139 and 21003097).

■ REFERENCES

- (1) Pratt, W. E.; Stevens, J. J.; Symons, P. G. *Polyaluminum chloride and aluminum chlorohydrate, processes and compositions: high-basicity and ultra high-basicity products*; U.S. Patent 7846318, 2010.
- (2) Zhang, W.-M.; Zhuang, J.-X.; Chen, Q.; Wang, S.; Song, W.-G.; Wan, L.-J. Cost-Effective Production of Pure Al_{13} from AlCl_3 by Electrolysis. *Ind. Eng. Chem. Res.* **2012**, *51* (34), 11201–11206.
- (3) Pletcher, D.; Walsh, F. *Industrial Electrochemistry*, 2nd ed.; Springer: New York, 1990.
- (4) Hind, A. R.; Bhargava, S. K.; Grocott, S. C. The surface chemistry of Bayer process solids: a review. *Colloids Surf., A* **1999**, *146* (1–3), 359–374.
- (5) Anastas, P. T.; Warner, J. C. *Green Chemistry: Theory and Practice*; Oxford University Press: New York, 2000.
- (6) Warner, J. C.; Cannon, A. S.; Dye, K. M. Green chemistry. *Environ. Impact Assess. Rev.* **2004**, *24* (7–8), 775–799.
- (7) Gunnarsson, S.; Soderlund, M. *Process for the production of polyaluminum salts*. U.S. Patent 20100170778, 2010.
- (8) Bertsch, P. M. Conditions for Al_{13} Polymer Formation in Partially Neutralized Aluminum Solutions. *Soil Sci. Soc. Am. J.* **1987**, *51* (3), 825–828.
- (9) Jia, Z.; He, F.; Liu, L. Synthesis of Polyaluminum Chloride with a Membrane Reactor: Operating Parameter Effects and Reaction Pathways. *Ind. Eng. Chem. Res.* **2004**, *43* (1), 12–17.
- (10) Casey, W. H. Large Aqueous Aluminum Hydroxide Molecules. *Chem. Rev.* **2006**, *106* (1), 1–16.
- (11) Park, K. Y.; Park, Y.-W.; Youn, S.-H.; Choi, S.-Y. Bench-Scale Decomposition of Aluminum Chloride Hexahydrate to Produce Poly(aluminum chloride). *Ind. Eng. Chem. Res.* **2000**, *39* (11), 4173–4177.
- (12) Hartman, M.; Trnka, O.; Šolcová, O. Thermal Decomposition of Aluminum Chloride Hexahydrate. *Ind. Eng. Chem. Res.* **2005**, *44* (17), 6591–6598.
- (13) Zhuang, J.-X.; Chen, Q.; Wang, S.; Zhang, W.-M.; Song, W.-G.; Wan, L.-J.; Ma, K.-S.; Zhang, C.-N. Zero discharge process for foil industry waste acid reclamation: Coupling of diffusion dialysis and electro dialysis with bipolar membranes. *J. Membr. Sci.* **2013**, *432*, 90–96.
- (14) He, F.; Jia, Z.; Wang, P.; Liu, Z. Synthesis of polyaluminum chloride with a membrane reactor: parameters optimization for the in situ synthesis. *J. Membr. Sci.* **2005**, *247* (1–2), 221–226.
- (15) He, F.; Wang, P.; Jia, Z.; Liu, Z. Synthesis of polyaluminum chloride with a membrane reactor: effects of operation modes. *J. Membr. Sci.* **2003**, *227* (1–2), 15–21.
- (16) Jaime-Ferrer, J. S.; Couallier, E.; Viers, P.; Rakib, M. Two-compartment bipolar membrane electro dialysis for splitting of sodium formate into formic acid and sodium hydroxide: Modelling. *J. Membr. Sci.* **2009**, *328* (1–2), 75–80.
- (17) Wang, Y.; Huang, C.; Xu, T. Which is more competitive for production of organic acids, ion-exchange or electro dialysis with bipolar membranes? *J. Membr. Sci.* **2010**, *374* (1–2), 150–156.
- (18) de Groot, M. T.; de Rooij, R. M.; Bos, A. A. C. M. Bargeman, G. Bipolar membrane electro dialysis for the alkalization of ethanolamine salts. *J. Membr. Sci.* **2011**, *378* (1–2), 415–424.

(19) ANSI/AWWA B408-10 *Liquid Polyaluminum Chloride*; American National Standards Institute: Washington, DC, 2010.

(20) Xue, Z.-X.; Wang, G.; Zhou, X.-Y. The characteristics and production ways of soluble aluminium hydroxide. *Light Met. (in Chinese)* **2011**, *1*, 20–22.

(21) Suzuki, T.; Tamagawa, S. *Aluminum hydroxide gel particle and production method thereof*. U.S. Patent 20130145965, 2013.

(22) Hem, J. D.; Roberson, C. E. *Form and Stability of Aluminum Hydroxide Complexes in Dilute Solution*; U.S. G.P.O.: Washington, DC, 1967.

(23) Teagarden, D. L.; Hem, S. L.; White, J. L. Conversion of aluminum chlorohydrate to aluminum hydroxide. *J. Soc. Cosmet. Chem.* **1982**, *33*, 281–295.

Online Supporting Information for

“Green Production of Ultrahigh-Basicity Polyaluminum Salts with Maximum Atomic Economy by Ultrafiltration and Electrodialysis with Bipolar Membranes”

*Qing Chen¹, Chang Xue¹, Wei-Ming Zhang*¹, Wei-Guo Song*², Li-Jun Wan² and Kun-Song Ma³*

¹ College of Chemistry & Materials Engineering, Wenzhou University, Wenzhou 325000, P.R. China

² Beijing National Laboratory for Molecular Sciences (BNLMS); Institute of Chemistry, Chinese Academy of Sciences, Beijing 100190, P.R. China

³ Yangzhou Hongyuan Electronic Co., Ltd., Gaoyou 225600, P.R. China

*Corresponding author. Tel.: +86 577 86689300 (W.-M. Zhang), +86 10 62557908 (W.-G. Song)

E-mail: weiming@iccas.ac.cn, wsong@iccas.ac.cn

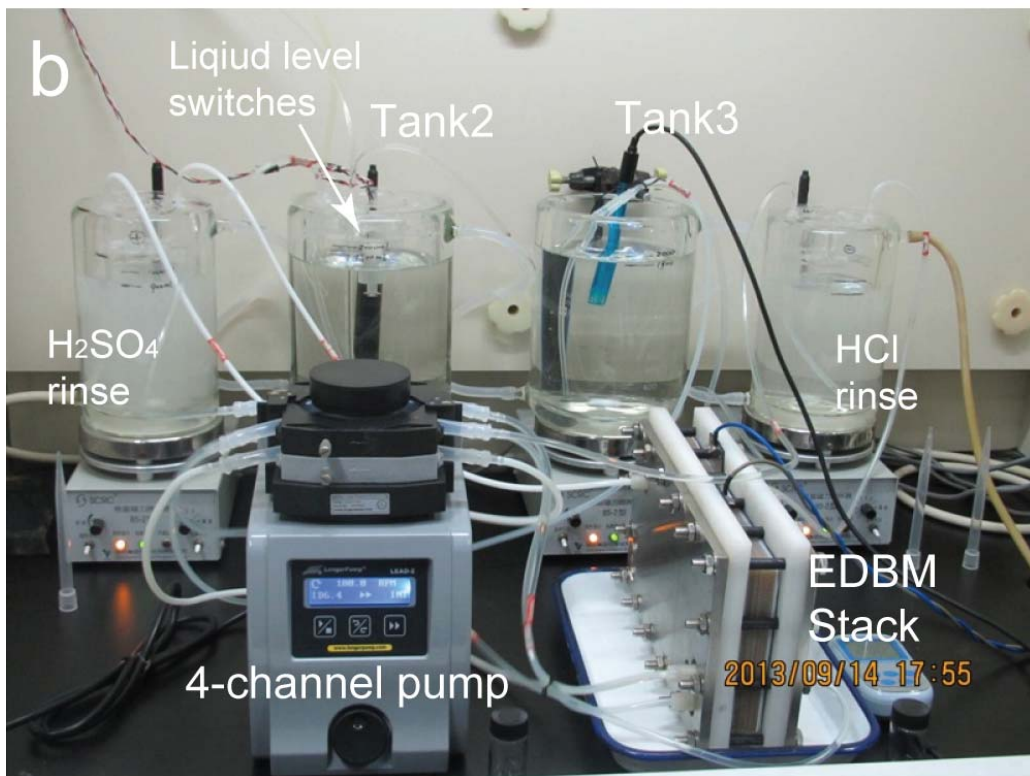
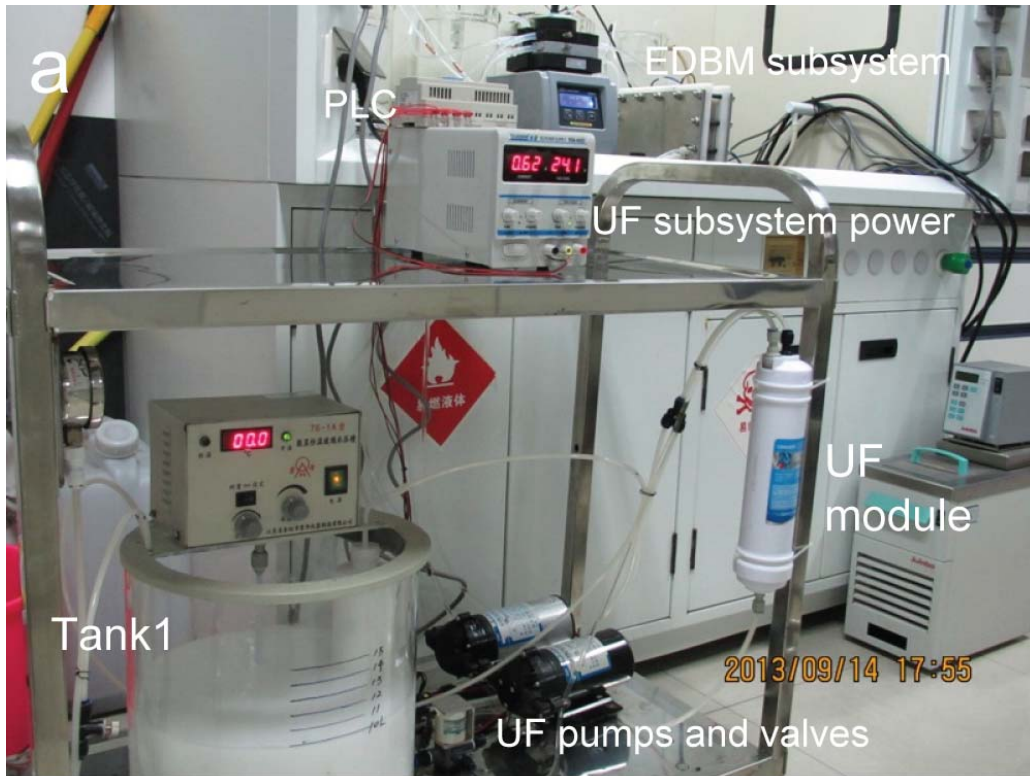


Figure S1. Photographs of the integrated system. The UF subsystem (a) and the EDBM subsystem (b).

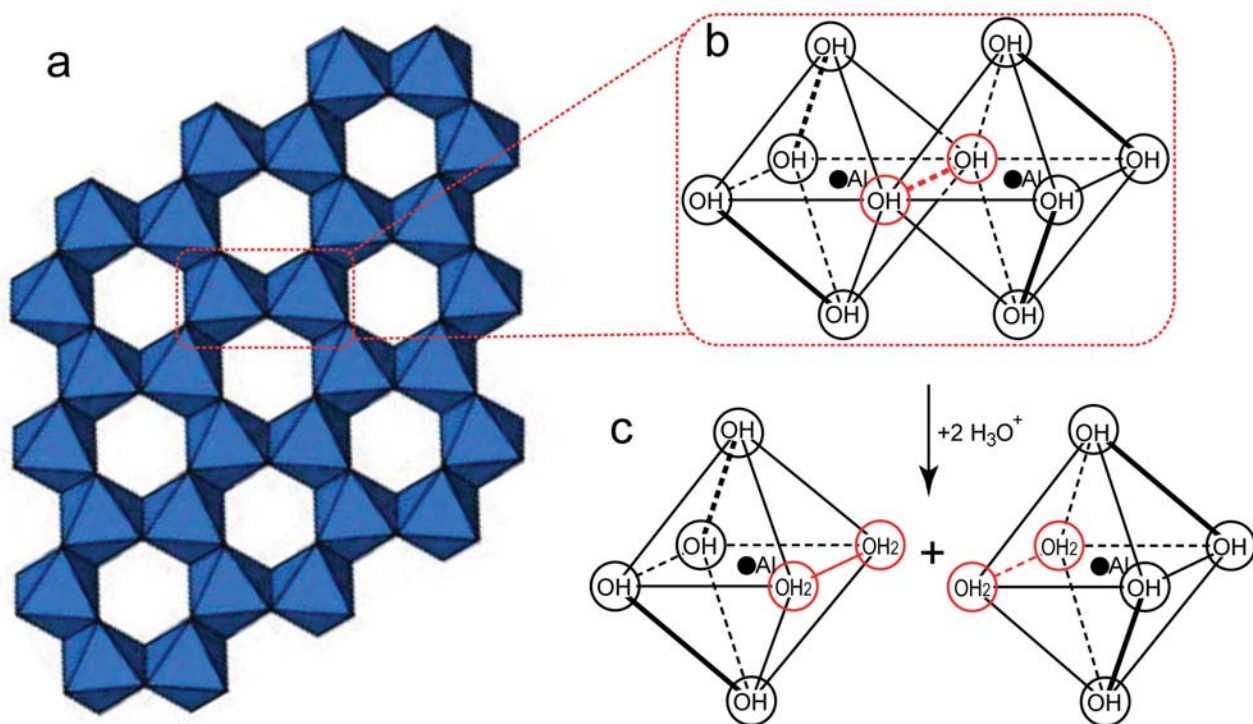


Figure S2. Solution chemistry of $\text{Al}(\text{OH})_3$ reacting with free acids. (a) Schematic layer structure of aluminum hydroxide (gibbsite). Each octahedron represents 1 Al^{3+} surrounded by 6 OH^- , and each OH^- is shared by 2 adjacent octahedrons, giving an empirical formula of $\text{Al}(\text{OH})_3$. (b) A close look of the adjacent aluminum octahedrons. The shared double hydroxide bridges are emphasized as thick lines. (c) The combined hydroxide bridges are taken apart when attacked by hydrated protons. Separated $[\text{Al}(\text{H}_2\text{O})_6]^{3+}$ octahedrons are the final products when gibbsite reacts with adequate free acids.

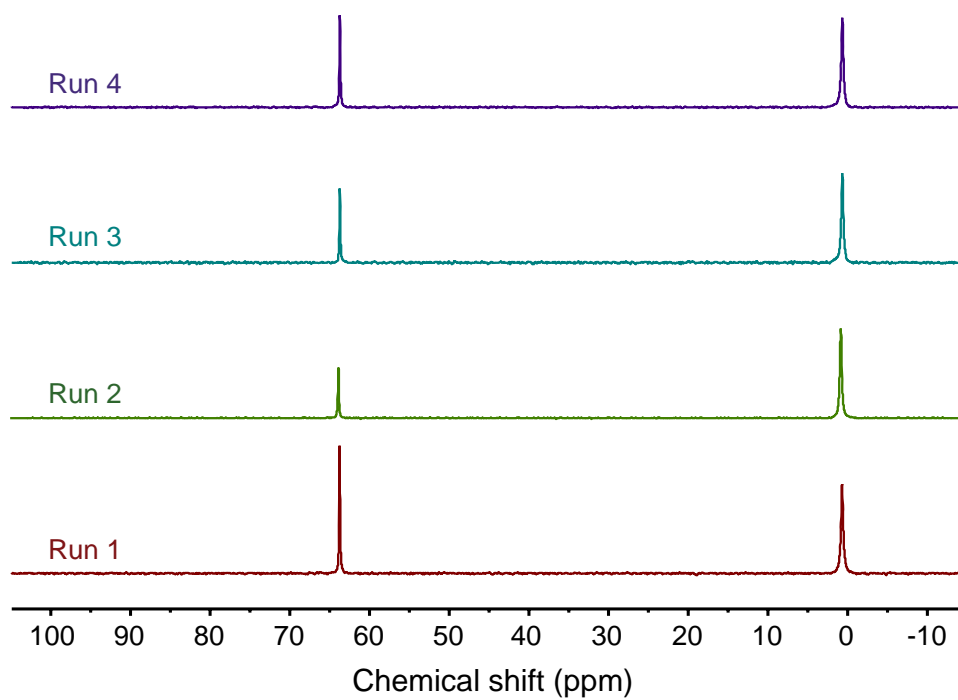


Figure S3. ^{27}Al -NMR spectrum of the final polyaluminum products in all batches.

Items	UF+EDBM process	Notes
Lab system parameters		
System production cycle	2.0 hour/batch	EDBM with large mixing tank, including 30 min clean
Final product basicity	70%	See Fig. 4c for details
Polyaluminum salt yield	0.90 mol/batch	Calculated as Al
	0.101 kg/batch	Calculated as $Al_2(OH)_{4.2}Cl_{1.8} \cdot 2H_2O$ solids
UF effective membrane area	0.20 m ²	
UF average power	20.0 W	15 W for normal and 40 W for flush operation
UF energy consumption	0.040 kWh/batch	
EDBM effective membrane area	0.168 m ²	187 cm ² x 9 cell pairs
EDBM energy consumption	0.250 kWh/batch	See Fig. 3b for details
Full system cost estimation		
Scale up factor from lab system	200	Cost analysis applicable for large system only
UF effective membrane area	40 m ²	
UF module cost	1,200 \$	Litree LH3-1060-V module (same fiber, 40 m ² area)
EDBM effective membrane area	33.7 m ²	
EDBM total membrane area	42.1 m ²	80% effective area ratio
BP membrane cost	30,294 \$	\$720/m ² for BP membrane
Anion membrane cost	15,147 \$	\$360/m ² for anion membrane
EDBM stack cost	68,162 \$	1.5 times for membranes
Cost for core membrane modules	69,362 \$	UF Module + EDBM stack
Peripheral equipment cost	34,681 \$	50% of core membrane modules
Capital cost	104,042 \$	
Maintenance cost	10,404 \$/year	10% of capital cost per year
System lifespan	2 year	
Available working time	8,000 hour/year	
Total investment in system lifespan	124,851 \$	Capital + Maintenance
Total yields in system lifespan	162,216 kg	as $Al_2(OH)_{4.2}Cl_{1.8} \cdot 2H_2O$ solids
Capital cost	0.770 \$/kg	
Energy consumption	2.86 kWh/kg	UF + EDBM
Electricity charge	0.10 \$/kWh	
Energy cost	0.286 \$/kg	
Total cost (exclude feed chemicals)	1.06 \$/kg	as $Al_2(OH)_{4.2}Cl_{1.8} \cdot 2H_2O$ solids

Table S1. Cost estimation of the integrated process.